

Changing climate both increases and decreases European river floods

Original

Changing climate both increases and decreases European river floods / Blöschl, Günter; Hall, Julia; Viglione, Alberto; Perdigão, Rui A P; Parajka, Juraj; Merz, Bruno; Lun, David; Arheimer, Berit; Aronica, Giuseppe T; Bilibashi, Ardian; Bohá, Milo; Bonacci, Ognjen; Borga, Marco; anjevac, Ivan; Castellarin, Attilio; Chirico, Giovanni B; Claps, Pierluigi; Frolova, Natalia; Ganora, Daniele; Gorbachova, Liudmyla; Gül, Ali; Hannaford, Jamie; Harrigan, Shaun; Kireeva, Maria; Kiss, Andrea; Kjeldsen, Thomas R; Kohnová, Silvia; Koskela, Jarkko J; Ledvinka, Ondrej; Macdonald, Neil; Mavrova-Guirquinova, Maria; Mediero, Luis; Merz, Ralf; Molnar, Peter; Montanari, Alberto; Murphy, Conor; Osuch, Marzena; Ouycharuk, Valeria; Radevski, Ivan; Salinas, José L; Sauquet, Eric; Šraj, Mojca; Szolgay, Jan; Volpi, Elena; Wilson, Donna; Zaimi, Klodian; Zivkovi, Nenad. - In: NATURE. - ISSN 0028-0836. - (2019). [10.1038/s41586-019-1495-6]

Publisher:

Springer Nature Publishing

Published

DOI:10.1038/s41586-019-1495-6

Terms of use:

This article is made available under terms and conditions as specified in the corresponding bibliographic description in the repository

Publisher copyright

(Article begins on next page)

Changing climate both increases and decreases European river floods

Günter Blöschl^{1†}, Julia Hall^{†1}, Alberto Viglione^{1, 12}, Rui A. P. Perdigão¹, Juraj Parajka¹, Bruno Merz², David Lun¹, Berit Arheimer³, Giuseppe T. Aronica⁴, Ardian Bilibashi⁵, Miloň Boháč⁶, Ognjen Bonacci⁷, Marco Borga⁸, Ivan Čanjevac⁹, Attilio Castellarin¹⁰, Giovanni B. Chirico¹¹, Pierluigi Claps¹², Natalia Frolova¹³, Daniele Ganora¹², Liudmyla Gorbachova¹⁴, Ali Gül¹⁵, Jamie Hannaford¹⁶, Shaun Harrigan¹⁷, Maria Kireeva¹³, Andrea Kiss¹, Thomas R. Kjeldsen¹⁸, Silvia Kohnová¹⁹, Jarkko J. Koskela²⁰, Ondrej Ledvinka⁶, Neil Macdonald²¹, Maria Mavrova-Guirguinova²², Luis Mediero²³, Ralf Merz²⁴, Peter Molnar²⁵, Alberto Montanari⁹, Conor Murphy²⁶, Marzena Osuch²⁷, Valeryia Ovcharuk²⁸, Ivan Radevski²⁹, José L. Salinas¹, Eric Sauquet³⁰, Mojca Šraj³¹, Jan Szolgay¹⁸, Elena Volpi³², Donna Wilson³³, Klodian Zaimi³⁴, and Nenad Živković³⁵

¹Institute of Hydraulic Engineering and Water Resources Management, Technische Universität Wien, Vienna, Austria

²Helmholtz Centre Potsdam, GFZ German Research Centre for Geosciences, Potsdam, Germany

³Swedish Meteorological and Hydrological Institute, Norrköping, Sweden

⁴Department of Engineering, University of Messina, Messina, Italy

⁵CSE – Control Systems Engineer, Renewable Energy Systems & Technology, Tirana, Albania

⁶Czech Hydrometeorological Institute, Prague, Czechia

⁷Faculty of Civil Engineering, Architecture and Geodesy, Split University, Split, Croatia

⁸Department of Land, Environment, Agriculture and Forestry, University of Padova, Padua, Italy

⁹University of Zagreb, Faculty of Science, Department of Geography, Zagreb, Croatia

¹⁰Department of Civil, Chemical, Environmental and Materials Engineering (DICAM), Università di Bologna, Bologna, Italy

¹¹Department of Agricultural Sciences, University of Naples Federico II, Naples, Italy

¹²Department of Environment, Land and Infrastructure Engineering (DIATI), Politecnico di Torino, Turin, Italy

¹³Department of Land Hydrology, Lomonosov Moscow State University, Moscow, Russia

¹⁴Department of Hydrological Research, Ukrainian Hydrometeorological Institute, Kiev, Ukraine

¹⁵Department of Civil Engineering, Dokuz Eylül University, Izmir, Turkey

¹⁶Centre for Ecology & Hydrology, Wallingford, Oxfordshire, UK

¹⁷Forecast Department, European Centre for Medium-Range Weather Forecasts (ECMWF), UK

¹⁸Department of Architecture and Civil Engineering, University of Bath, Bath, UK

¹⁹Slovak University of Technology in Bratislava, Faculty of Civil Engineering, Department of Land and Water Resources Management, Bratislava, Slovakia

²⁰Finnish Environment Institute, Helsinki, Finland

²¹Department of Geography and Planning & Institute of Risk and Uncertainty, University of Liverpool, Liverpool, UK

²²University of Architecture, Civil Engineering and Geodesy, Sofia, Bulgaria

²³Department of Civil Engineering: Hydraulic, Energy and Environment, Universidad Politécnica de Madrid, Madrid, Spain

²⁴Department for Catchment Hydrology, Helmholtz Centre for Environmental Research – UFZ, Halle, Germany

²⁵Institute of Environmental Engineering, ETH Zurich, Zurich, Switzerland

²⁶Irish Climate Analysis and Research Units (ICARUS), Department of Geography, Maynooth University, Ireland

²⁷Department of Hydrology and Hydrodynamics, Institute of Geophysics Polish Academy of Sciences, Warsaw, Poland

²⁸Hydrometeorological Institute, Odessa State Environmental University, Odessa, Ukraine

²⁹Institute of Geography, Faculty of Natural Sciences and Mathematics, Ss. Cyril and Methodius University, Skopje, Republic of Macedonia

³⁰Irstea, UR RiverLy, Lyon-Villeurbanne, France

³¹University of Ljubljana, Faculty of Civil and Geodetic Engineering, Ljubljana, Slovenia

³²Department of Engineering, University Roma Tre, Rome, Italy

³³Norwegian Water Resources and Energy Directorate, Oslo, Norway

³⁴Institute of Geo-Sciences, Energy, Water and Environment (IGEWE), Polytechnic University of Tirana, Tirana, Albania

³⁵University of Belgrade, Faculty of Geography, Belgrade, Serbia

* e-mail: bloeschl@hydro.tuwien.ac.at

† These authors contributed equally to this work.

Abstract

Climate change has led to concerns of increasing river floods resulting from the greater water holding capacity of a warmer atmosphere¹. This concern is reinforced by evidence of increasing economic losses in many parts of the world, including Europe². Any changes in river floods would have lasting implications for designing flood protection measures and for flood risk zoning. Existing studies have been unable to identify a consistent continental-scale climatic change signal in flood discharge observations in Europe³, because of limited spatial coverage and choices in the grouping of hydrometric stations. Here we show that clear regional patterns of both increases and decreases in observed river flood discharges in the last five decades in Europe are evident, which are likely manifestations of a changing climate. Our results suggest that (i) increasing autumn and winter rainfall has led to increasing floods in northwestern Europe, (ii) decreasing precipitation and increasing evaporation have led to decreasing floods in medium and large catchments in southern Europe and (iii) decreasing snowcover and snowmelt as a result of warmer temperatures have led to decreasing floods in eastern Europe. Regional flood discharge trends in Europe range from an increase of +11.4% per decade to a decrease of -23.1%. Notwithstanding the spatial and temporal heterogeneity of the observational record, the flood changes identified here are broadly consistent with climate model projections for the next century^{4,5}, suggesting that climate-driven changes are already happening, which supports calls for future climate change consideration in flood risk management.

River floods are among the most costly natural hazards. Global annual average losses are estimated at US \$104 billion⁶, and are expected to increase as a result of economic growth, urbanization and climatic change^{2,7}. Physical arguments of increased heavy precipitation resulting from the enhanced water holding capacity in a warmer atmosphere and the occurrence of numerous large floods have exacerbated concerns of increasing flood magnitudes¹. However, observations of individual extreme events do not necessarily imply that the long-term statistics of flood discharge are also increasing³.

In Europe, a climatic change signal in flood discharges over the past five decades has been demonstrated in relation to changes in timing of floods within the year⁸. For example, in northeastern Europe, warmer air temperatures have led to earlier spring snowmelt floods. However, changes in flood discharges are still contested, as no coherent large-scale observational evidence has to date been available at the continental scale, as a result of limited spatial coverage and choices in the grouping of hydrometric stations³. A number of studies point towards increases in flood discharges in western Europe in the past five decades. The findings include upward trends in flood discharges in 15% of the stations⁹, an increase in the occurrence of extreme flood discharges by 44%¹⁰, and significant increases in major-flood occurrence in medium sized catchments¹¹. However, these studies are not fully representative as the stations are mainly clustered around western Europe.

Here we analyze the most comprehensive data set of flood observations in Europe¹² to show that a changing climate has increased river flood discharges in some regions of Europe, but decreased floods in others. We base our analysis on river discharge observations from 3738 gauging stations for the period 1960–2010. The catchment areas range between 5 and 100,000 km². For each station, we extracted a series consisting of the highest peak discharge recorded in each calendar year, the annual maximum peak flow. We estimated the trend in each series using the Theil-Sen slope estimator, tested the statistical significance with the Mann-Kendall test, and estimated regional trends by spatial interpolation. We also derived the long-term evolution of floods using a 10-year moving average filter. Finally, we analyzed in a similar fashion the change signal of three plausible drivers of floods: annual maximum 7-day precipitation; highest monthly soil moisture in each year; and spring (January to April) mean air temperature as a proxy for snowmelt and snowfall-to-rain transition. We examined the consistency of the changes in the drivers with those of the floods by comparing the change patterns and by Spearman rank correlation coefficients.

Our data show a clear regional pattern in flood trends across Europe (Fig. 1). Regional trends, relative to the mean flood discharges over 1960–2010, range from an increase of +11.4% to a decrease of -23.1% per decade (Fig. 1). The uncertainties of the regional trends (Extended Data Fig. 2b) are small (typically between 1 and 2% per decade) relative to the spatial signal. Local trends (Extended Data Fig. 2a) at the stations range from an increase of +17.8% to a decrease of -28.8% of the long-term station mean per decade. The spatial patterns of trends are grouped into three main regions. In northwestern Europe (Fig. 1, region 1), ~69% of stations show an increasing flood trend (Extended Data Table 2a) with an average local increase of +2.3% per decade. In southern Europe (Fig. 1, region 2), ~74% of stations show a decreasing trend with a regional average trend of -5% per decade. In eastern Europe (Fig. 1, region 3), ~78% of stations show a decreasing flood trend with an average decrease of -6% per decade. In northern Scandinavia and northwestern Russia, trends are less pronounced.

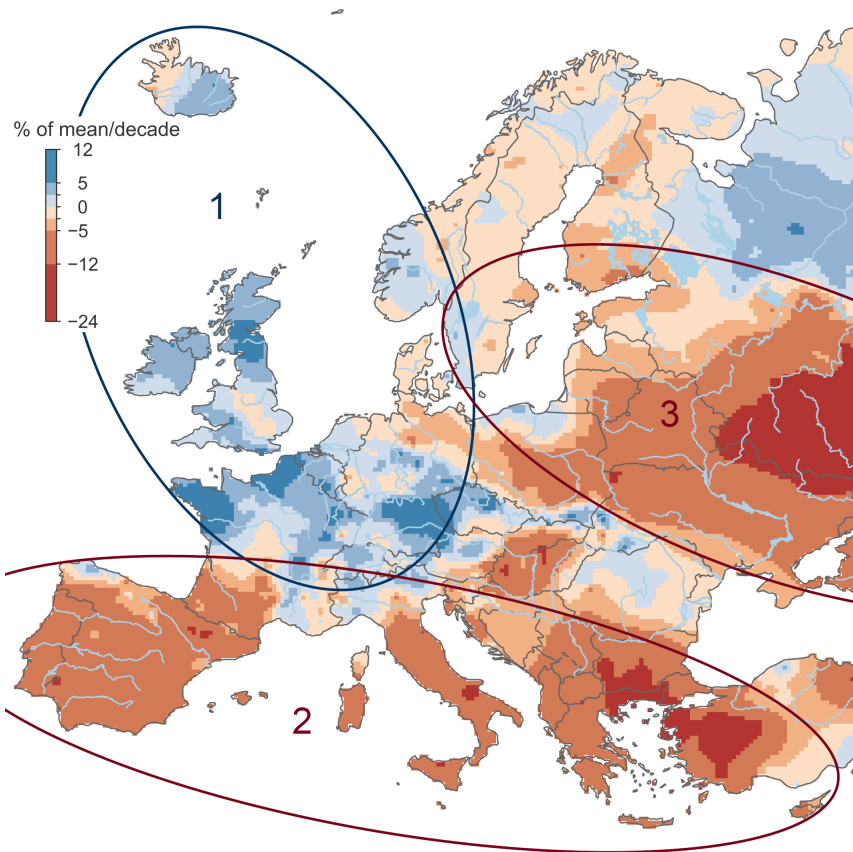


Fig. 1 | Observed regional trends of river flood discharges in Europe (1960–2010). Blue indicates increasing flood discharges, red decreasing flood discharges (percentage change per decade of the mean annual flood discharge). No. 1–3 indicate regions with distinct drivers: [1] northwestern Europe: increasing rainfall and soil moisture; [2] southern Europe: decreasing rainfall and increasing evaporation; [3] eastern Europe: decreasing and earlier snowmelt. The trends are based on $n = 2370$ hydrometric stations. For uncertainties see Extended Data Fig. 2b.

To interpret these changes we focused on seven hotspots of change, where flood trends are particularly clear and flood processes are broadly similar⁸ (Extended Data Fig. 2). Because floods result from the interaction between precipitation, soil moisture and snowmelt, we analyzed the temporal evolution of these drivers, using air temperature as a surrogate for snowmelt, and compared them to that of floods (Extended Data Fig. 4 a–g). Depending on the region, some of these drivers can be more important than others in explaining flood changes⁸.

In northern UK, floods predominantly result from winter rains associated with high soil moisture¹⁴ (Extended Data Fig. 4a). The increase in the flood discharges therefore closely follows increases in winter rainfall and to some degree that of soil moisture (Fig. 2a). This is also shown by statistically significant positive correlations between the temporal variability of flood discharges and these two drivers (Spearman rank correlation coefficient $r = 0.70$ and 0.36 , respectively, Table 1). In western France (Fig. 2b), southern Germany and western Czechia (Fig. 2c), increases in floods are also associated with increases in rainfall, although the correlation with soil moisture is stronger than in the UK, reflecting the important role of soil moisture in flood generation during spring and summer¹⁵ (Extended Data Fig. 4 a–c). In northern Iberia (Fig. 2d), decreasing floods are mainly caused by decreasing winter rainfall, amplified by decreasing soil moisture linked to increasing evapotranspiration¹⁶. Similarly, in the central Balkans (Fig. 2e), floods have decreased over most of the study period as a result of decreasing precipitation and soil moisture, but the trend appears to have reversed in the 1990s. In southern Finland (Fig. 2f) and western Russia (Fig. 2g), floods usually occur in spring¹⁷, and snowmelt plays an important role. The data show that air temperature

has strongly increased (more than 0.5°C per decade) and spring and early summer flood discharges have decreased ($r = -0.34$ and -0.55 , respectively, Table 1), reflecting shallower snow packs, earlier spring thaw (Extended Data Fig. 4f-g), and decreasing snowmelt.

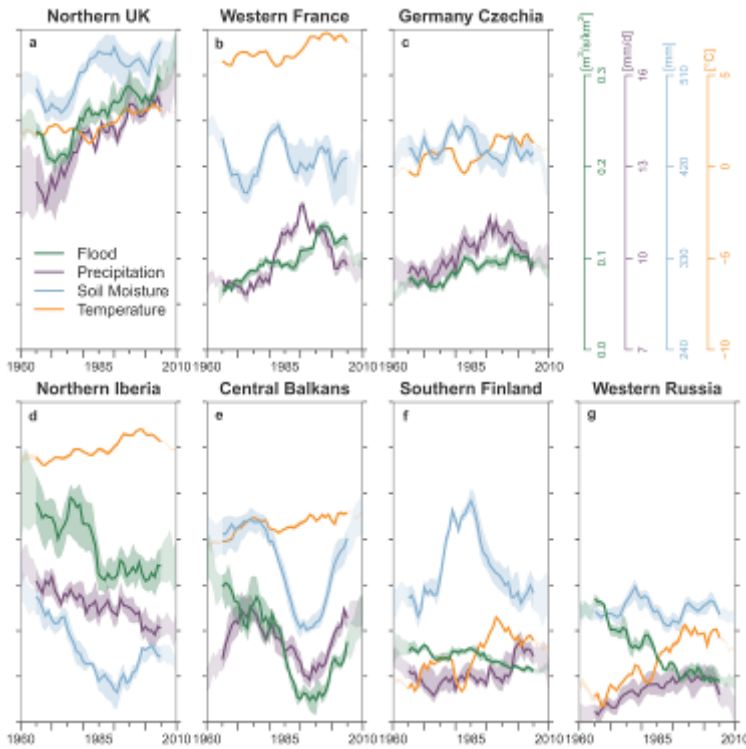


Fig. 2 | Long-term temporal evolution of flood discharges and their drivers for seven hotspots in Europe. (a) Northern UK, (b) Western France (c) Southern Germany and Western Czechia, (d) Northern Iberia, (e) Central Balkans, (f) Southern Finland, (g) Western Russia. Observed floods (green), maximum 7-day precipitation (purple), maximum monthly soil moisture (blue), and mean spring air temperature (orange). Solid lines show the median and shaded bands indicate the spatial variability within the hotspots (25th and 75th percentile). All data were subjected to a 10-year moving average filter. Vertical axes are indicated in top right corner.

Table 1 | Spearman's rank correlation coefficient (r) between hotspot medians of the annual series of flood discharge and their drivers. Confidence bounds of r are given in Extended Data Table 2b.

	Northern UK	Western France	Germany Czechia	Northern Iberia	Central Balkans	Southern Finland	Western Russia
Precipitation	0.70 **	0.41 *	0.40 *	0.54 **	0.22	0.08	-0.13
Soil Moisture	0.36 *	0.57 **	0.56 **	0.37 *	0.68 **	0.20	0.30
Spring temperature	0.09 †	0.50 ** †	0.04	0.02	-0.29	-0.34	-0.55 **

[(**) p -value < 0.001, (*) p -value < 0.01, † Little snow influence on floods. Bold print indicates largest correlation coefficients in each hotspot.]

In northwestern Europe (Fig. 1, region 1), increases in extreme precipitation (Fig. 2a-c; Extended Data Fig. 5b) are related to the poleward shift of the subpolar jet and associated storm tracks observed since the 1970s associated with more prevalent positive phases of the North Atlantic Oscillation (NAO) and polar warming¹⁸. The relationship of NAO variability with polar warming is still debated. Floods in the northern UK hotspot are closely aligned with increasing precipitation resulting in a mean flood discharge trend of +6.6% (Extended Data Table 2c).

125 In southern Europe (Fig. 1, region 2), the northward shift of the subtropical jet and associated storm
126 tracks¹⁹ as a result of the expansion of the Hadley cell²⁰ has led to decreasing precipitation, which,
127 together with increasing evapotranspiration¹⁶ related to warmer temperatures, has substantially
128 reduced soil moisture by around 5% per decade (Extended Data Figs. 5b,6b,7b). The combined
129 effect has resulted in decreasing flood discharges in the catchments analyzed here. Small
130 catchments of a few square kilometers are not contained in the data set (the median catchment size
131 of region 2 is about 400 km²), as they are usually not monitored or the flood series are too short for
132 trend analyses. In small catchments, local short-duration convective storms with high intensities are
133 more relevant for flood generation than long-duration synoptic storms, which produce floods in
134 medium and large catchments contained in the data²¹. Local convective storms are expected to
135 increase in a warmer climate²², which means that floods in small catchments may have actually
136 increased. Additionally, soil compaction, abandoned terraces and land-cover changes may increase
137 flood discharges in small catchments²³. The difference in catchment size may explain the apparent
138 inconsistency between the occurrence of numerous floods in small catchments in recent years in
139 southern Europe²¹ and the decreasing trend in Fig. 1.

140
141 In all but southern Europe, increases in extreme precipitation (Fig. 2a–c,f,g; Extended Data Fig. 5b)
142 are related to increased atmospheric blocking associated with decreasing pressure differences
143 between Greenland and the Baltic, which has decreased the speed of zonal (west-east) flow and
144 increased the chance of standing planetary waves²⁴. However, it is only in northwestern Europe (Fig.
145 1, region 1), where the increase in extreme precipitation is reflected in increased flood discharges,
146 as winter storms in that region cause winter floods⁸. Further in the east, snowmelt is more relevant
147 for flood generation.

148
149 In eastern Europe, spring air temperature has increased by as much as 1°C per decade (Extended
150 Data Fig. 6b). This has resulted in much less extensive spring snow cover²⁵, a shift of snowfall to
151 rainfall when air temperatures are around zero, shallower snow packs, earlier snowmelt⁸, likely
152 increased infiltration resulting from shallower freezing depths and therefore smaller floods, even
153 though extreme precipitation in summer has increased²⁶. The mean flood trend in the western
154 Russian hotspot is -18.2% (Extended Data Table 2c). Given the colder background temperature
155 (Extended Data Fig. 6a) and larger snowpack in northwestern Russia, the increasing temperatures
156 are not yet changing snowmelt patterns, and hence not decreasing floods (Fig. 1).

157
158 While past studies have focused on a few catchments or were clustered around western Europe^{9–11,27},
159 this study provides a continental perspective, which allows for an analysis of climate processes that
160 manifest themselves at larger scales. Isolated local or national scale studies, however, are broadly
161 consistent with our findings.

162
163 Our results have implications for flood risk management in medium and large sized catchments.
164 The trends shown in Fig. 1 are estimates of changes in the mean annual flood. Since mean annual
165 floods and more extreme floods are usually closely correlated²⁸, similar trends could also be
166 expected for the 100-year flood, which is often the key design criterion in flood risk management.
167 In northwest Europe (Fig. 1, region 1), flood discharges per unit catchment area (specific flood
168 discharges) are generally high (Fig. 3). For example, on the west coast of the British-Irish Isles and
169 Norway, the specific 100-year flood discharge during the period 1960-2010 was ~0.9 (m³/s)/km²
170 (Fig. 3), with floods increasing by ~5% per decade. However, in eastern Europe (Fig 1, region 3),
171 specific flood discharges are rather small (Fig. 3), and are likely to become smaller in a changing
172 climate. For example, in the Baltic countries, southern Poland and the Ukraine, the 100-year flood
173 of ~0.1 (m³/s)/km² would decrease to ~0.075 (m³/s)/km² if the observed decrease of ~5% per decade
174 persists over the next 50 years. In southern Europe, even if flood discharges decrease in medium
175 and large catchments, discharges are still generally high (Fig. 3), as a result of the proximity to the

Mediterranean Sea and associated heavy precipitation events²⁹. Floods in small catchments may actually increase as a result of enhanced convective storms³⁰ and land-use change²³.

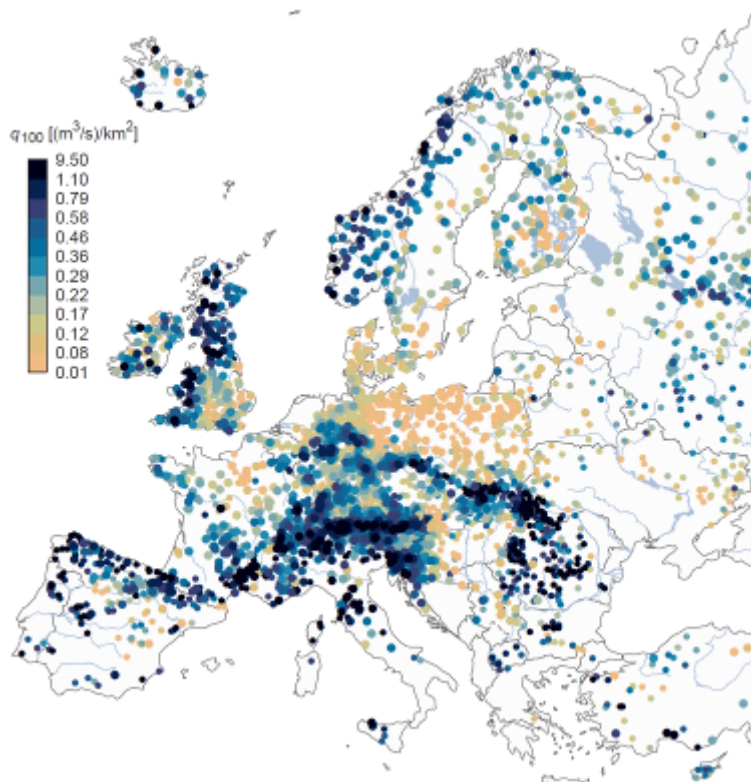


Fig. 3 | Specific 100-year floods ((m³/s)/km²) in Europe, where larger points indicate 90% confidence intervals smaller than 60% of the estimate.

Increasing flood discharges imply that, the 100-year flood discharge five decades ago, now has a smaller return period than 100 years, i.e. that discharge is likely to be exceeded on average more often than once in 100 years. In northwestern Europe, what was the 100-year flood discharge in 1960 has now typically become a 50- to 80-year flood discharge (Extended Data Fig. 8), which will make flood defense structures less safe. In eastern Europe, the 100-year flood discharge has now become a 125- to 250-year flood discharge, which will make structures less economical. While Extended Data Fig. 8, and Fig. 3, do provide a continental overview, they do not replace national-scale and local studies where more detailed information may be available.

It should be noted that the flood trends observed here do not necessarily extrapolate into the future as they may be related to climate variability rather than persistent changes in time¹¹. Also, the trends depend on the observation period³, so may differ if the observation period is extended. However, the regions with a distinct climatic change signal in observed flood discharges identified here are broadly coherent with the projected flood changes in Europe. Most projections for the end of the 21st century suggest increasing floods in (north)western Europe due to increasing precipitation, and decreasing floods in eastern and northern Europe due to increasing temperatures^{4,5}. This means that changes in flood discharge magnitudes are already underway, which adds credence to those projections and supports the need to account for climate induced changes in flood risk management.

References:

1. IPCC. *Managing the Risks of Extreme Events and Disasters to Advance Climate Change Adaptation. A Special Report of Working Groups I and II of the Intergovernmental Panel on*

- 207 *Climate Change*. (Cambridge University Press, Cambridge, UK and New York, NY, USA,
208 2012).
- 209 2. EASAC. European Academies' Science Advisory Council Statement; Extreme weather events
210 in Europe - Preparing for climate change adaptation: an update on EASAC's 2013 study. at
211 <<https://easac.eu/publications/details/extreme-weather-events-in-europe/>>
- 212 3. Hall, J. *et al.* Understanding flood regime changes in Europe: a state of the art assessment.
213 *Hydrol. Earth Syst. Sc.* **18**, 2735–2772 (2014).
- 214 4. Kundzewicz, Z. *et al.* Differences in flood hazard projections in Europe-their causes and
215 consequences for decision making. *Hydrol. Sci. J.* **62**, 1–14 (2017).
- 216 5. Thober, S. *et al.* Multi-model ensemble projections of European river floods and high flows at
217 1.5, 2, and 3 degrees global warming. *Environ. Res. Lett.* **13**, 014003 (2018).
- 218 6. UNISDR. *Making Development Sustainable: The Future of Disaster Risk Management. Global*
219 *Assessment Report on Disaster Risk Reduction*. (Geneva, Switzerland: United Nations
220 International Strategy for Disaster Reduction (UNISDR), 2015).
- 221 7. Winsemius, H. C. *et al.* Global drivers of future river flood risk. *Nat. Clim. Chang.* **6**, 381–385
222 (2016).
- 223 8. Blöschl, G. *et al.* Changing climate shifts timing of European floods. *Science* **357**, 588–590
224 (2017).
- 225 9. Mangini, W. *et al.* Detection of trends in magnitude and frequency of flood peaks across
226 Europe. *Hydrol. Sci. J.* **63**, 493–512 (2018).
- 227 10. Berghuijs, W., Aalbers, E., Larsen, J., Trancoso, R. & Woods, R. Recent changes in extreme
228 floods across multiple continents. *Environ. Res. Lett.* **12**, (2017).
- 229 11. Hodgkins, G. A. *et al.* Climate-driven variability in the occurrence of major floods across North
230 America and Europe. *J. Hydrol.* **552**, 704–717 (2017).
- 231 12. Hall, J. *et al.* A European Flood Database: facilitating comprehensive flood research beyond
232 administrative boundaries. *Proc. Int. Assoc. Hydrol. Sci.* **370**, 89–95 (2015).
- 233 13. Sivapalan, M., Blöschl, G., Merz, R. & Gutknecht, D. Linking flood frequency to long-term
234 water balance: Incorporating effects of seasonality. *Water Resour. Res.* **41**, W06012 (2005).
- 235 14. Bayliss, A. C. & Jones, R. C. *Peaks-over-threshold flood database: Summary statistics and*
236 *seasonality. IH Report No. 121*. (Institute of Hydrology, Wallingford, UK, 1993).
- 237 15. Schröter, K., Kunz, M., Elmer, F., Mühr, B. & Merz, B. What made the June 2013 flood in
238 Germany an exceptional event? A hydro-meteorological evaluation. *Hydrol. Earth Syst. Sc.* **19**,
239 309–327 (2015).
- 240 16. Mediero, L., Santillán, D., Garrote, L. & Granados, A. Detection and attribution of trends in
241 magnitude, frequency and timing of floods in Spain. *J. Hydrol.* **517**, 1072–1088 (2014).
- 242 17. Hall, J. & Blöschl, G. Spatial patterns and characteristics of flood seasonality in Europe.
243 *Hydrol. Earth Syst. Sc.* **22**, 3883–3901 (2018).
- 244 18. IPCC. *2013: Climate Change 2013: The Physical Science Basis. Contribution of Working*
245 *Group I to the Fifth Assessment Report of the Intergovernmental Panel on Climate Change*.
246 (Cambridge University Press, Cambridge, UK and New York, USA, 2013).
- 247 19. Archer, C. L. & Caldeira, K. Historical trends in the jet streams. *Geophys. Res. Lett.* **35**, (2008).
- 248 20. Kang, S. M. & Lu, J. Expansion of the Hadley cell under global warming: Winter versus
249 summer. *J. Clim.* **25**, 8387–8393 (2012).
- 250 21. Amponsah, W. *et al.* Integrated high-resolution dataset of high-intensity European and
251 Mediterranean flash floods. *Earth Syst. Sci. Data* **10**, 1783–1794 (2018).
- 252 22. Ban, N., Schmidli, J. & Schär, C. Heavy precipitation in a changing climate: Does short-term
253 summer precipitation increase faster? *Geophys. Res. Lett.* **42**, 1165–1172 (2015).
- 254 23. Rogger, M. *et al.* Land-use change impacts on floods at the catchment scale - Challenges and
255 opportunities for future research. *Water Resour. Res.* **53**, 5209–5219 (2017).
- 256 24. Perdigão, R. A. P., Pires, C. A. L. & Hall, J. Synergistic Dynamic Theory of Complex
257 Coevolutionary Systems: Disentangling Nonlinear Spatiotemporal Controls on Precipitation.
258 *arXiv:1611.03403 [math.DS]* (2016).

- 259 25. Estilow, T. W., Young, A. H. & Robinson, D. A. A long-term Northern Hemisphere snow cover
260 extent data record for climate studies and monitoring. *Earth Syst. Sci. Data* **7**, 137–142 (2015).
261 26. Frolova, N. L. *et al.* Hydrological hazards in Russia: origin, classification, changes and risk
262 assessment. *Nat. Hazards* **88**, 103–131 (2017).
263 27. Mediero, L. *et al.* Identification of coherent flood regions across Europe by using the longest
264 streamflow records. *J. Hydrol.* **528**, 341–360 (2015).
265 28. Salinas, J. L., Castellarin, A., Kohnova, S. & Kjeldsen, T. Regional parent flood frequency
266 distributions in Europe-Part 2: Climate and scale controls. *Hydrol. Earth Syst. Sc.* **18**, 4391–
267 4401 (2014).
268 29. Xoplaki, E., Gonzalez-Rouco, J. F., Luterbacher, J. & Wanner, H. Wet season Mediterranean
269 precipitation variability: influence of large-scale dynamics and trends. *Clim. Dynam.* **23**, 63–78
270 (2004).
271 30. Brooks, H. E. Severe thunderstorms and climate change. *Atmos. Res.* **123**, 129–138 (2013).
272

Methods

Data sets

The hydrological data used in this study were obtained from a newly created European Flood Database¹², with subsequent updates, containing data from 3738 hydrometric gauging stations from 68 European data sources for the period 1960 to 2010 (Extended Data Table 1). Choice of the study period was guided by a tradeoff between data availability in terms of record length and spatial coverage. The database consists of the highest discharge (daily mean or instantaneous discharge) in each calendar year for each station. For consistency, we chose to analyze the annual maximum flood rather than multiple floods within a year in all stations, as in many areas only annual maxima were available. The stations are located within the domain bounded by 22.25 W – 60.25 E and 34.25 N – 71.25 N (Extended Data Fig. 1), and catchment areas range between 5 and 100,000 km².

The data set was screened for data errors, and catchments that were known, or were identified, to have experienced strong human modifications such as reservoirs that could affect changes in flood discharges were excluded. The screening involved data pre-selection by co-authors and additional visual examination of the flood records in question, analysis of flood seasonality (jumps in timing and large differences to surrounding stations), and examination of the catchment area in google maps. While local human effects on the floods of individual stations cannot be excluded, the focus of this study was on regionally consistent patterns of change where such effects will not be relevant. In a few catchments, the available flood data had been corrected for the effects of reservoirs to represent near natural flood discharge. In a few cases, local reservoirs may influence the data, but this does not affect the regional pattern. The station density is rather uneven (Extended Data Fig. 1b). In southern Europe it is lower as some stations were removed because of reservoir effects. In Italy, reduced record lengths are related to organizational changes of the hydrographic services¹². In eastern Europe the density of available stations is generally lower than in other countries and, again, some stations were removed because of reservoir effects.

For estimating the flood discharge trends (Fig. 1 and 2, Extended Data Fig. 2 and 8), only stations that satisfied the following three criteria were considered: at least 40 years of data were available during 1960–2010, the record started in 1968 or earlier, and ended in 2002 or later. In the countries with the highest station densities (Austria, Germany, Switzerland), only stations with at least 49 years of data were included in order to obtain a more even spatial distribution across Europe. In Cyprus, Italy and Turkey, stations with at least 30 years of data were included, and in Spain 40 years of data without restrictions to the start and end of the record. This selection resulted in a set of 2370 stations with a median catchment size of 381 km². Sensitivity analyses indicated that the large-scale spatial pattern of increasing and decreasing flood trends across Europe is not influenced by the choice of record length although the trend of individual stations tends to be sensitive to record length, when increasing the required record length by 5 years, the percentage of significantly positive and negative trends (Extended Data Table 2a) changes only slightly from respectively 11.52% and 16.50% to 11.04% and 16.95%. In this study we evaluated linear trends of the flood discharges. Alternative models of change (e.g. step changes) could also be tested but are beyond the scope of this study.

For each hydrometric gauging station, the contributing catchment boundary was derived from the CCM River and Catchment Database³¹. Daily gridded precipitation sum and mean air temperature data from the E-OBS data set (Version 17.0)³² for the period 1960–2010 were used. The data consist of interpolated ground-based observations with a spatial resolution of 0.25°. Monthly gridded soil moisture data from the CPC Soil Moisture data set³³ for the period 1960–2010 were analyzed. The data are model-calculated monthly averaged soil moisture water-height equivalents with a spatial resolution of 0.5°.

Analysis method

As a first step, we estimated the discharge trend by the Theil-Sen slope estimator^{34,35}. The trend estimator β is the median slope calculated using the differences of discharge Q over all possible pairs of years (i and j , $i < j$) within the time series,

$$\beta = \text{median}\left(\frac{Q_j - Q_i}{j - i}\right) \quad (1)$$

where β has units of m³/s per year, which was plotted as percentage of the mean flood discharge per decade in Extended Data Fig. 2. The trends were tested for significance by the Mann-Kendall test³⁶ (Extended Data Table 2a). Some false positives, i.e. detected trends where no trend is present, would be expected because of the large number of stations. The Mann-Kendall test requires the flood discharges to be temporally independent. We therefore tested whether lag 1 autocorrelation exists in the residuals from the trends. 92% of the stations did not exhibit significant lag 1 autocorrelation at the 5% level, suggesting that the Mann-Kendall test is applicable. To identify regional spatial patterns within Europe, β was spatially interpolated using the *autoKrige* function (automatic kriging) of the R *automap* package³⁷. The derived trend patterns are plotted in Fig. 1 and in the background of Extended Data Fig. 2a. The uncertainty of the estimated trends at the stations was estimated by bootstrapping⁴⁰ and is shown as points in Extended Data Fig. 2b. The uncertainty of the regional trends was estimated as the block kriging standard deviation (kriging error) using the *autoKrige* function and is shown in the background of Extended Data Fig. 2b. The variogram estimated by the function is

$$\gamma(h) = c_0 + c_1 \left(1 - \frac{1}{2^{v-1}\Gamma(v)} \left(\frac{h}{r}\right)^v K_v\left(\frac{h}{r}\right)\right) \quad (2)$$

where h is lag, $c_0 = 10.061$ (%/decade)², $c_1 = 57.708$ (%/decade)², $r = 2394.4$ km, $v = 0.2$ and K_v is the modified Bessel function of the second kind. We used block kriging rather than ordinary kriging as we are interested in the uncertainty of the regional estimate rather than that of the local estimate. The uncertainty is evaluated at a 200 x 200 km block size which is the scale at which we suggest Fig. 1 and Extended Data Fig. 2a to be read.

In order to evaluate the robustness of the spatial trend patterns we repeated the interpolation, however, only using stations with significant trends (Extended Data Fig. 3a). The overall pattern is similar to that of the interpolation using all stations (Extended Data Fig. 2a). Additionally, we repeated the interpolation but only using randomly selected stations with distances from each other larger than 50 km to examine the effect of spatial correlations on the trends (Extended Data Fig. 3b). Again, the patterns are similar.

As a second step, we selected rectangular areas or hotspots of change based on similarity of discharge trends and average flood timing as a proxy for flood processes (Extended Data Fig. 2, Extended Data Table 2c). We standardized the flood series of individual stations to zero mean and unit variance to make flood changes within hotspots comparable,

$$Q_{i,k}^0 = \frac{Q_{i,k} - \mu_{Q_k}}{\sigma_{Q_k}} \quad (3)$$

where μ_{Q_k} and σ_{Q_k} are the mean and the standard deviation of station k , respectively. To compare results between the hotspots we denormalised the flood series of each hotspot h by the mean specific flood discharge μ_h ((m³/s)/km²) over all years, and the square root σ_h of the mean temporal variance,

$$Q_{i,k}^* = \sigma_h Q_{i,k}^0 + \mu_h \quad (4)$$

and estimated the long-term evolution in flood discharge with a centered 10-year moving averaging window. We plotted the median of these series within each hotspot (solid lines) and 25th and 75th percentiles of all stations in that hotspot (shaded bands) in Fig. 2. Additionally, the original local flood discharges were tested for significance of a general trend in each hotspot by the Regional

Mann-Kendall test³⁸ (Extended Data Table 2c). Names of hotspots are only indicative and do not correspond to any exactly defined geographic area.

To investigate rain-induced effects on flood changes, we identified for each grid point of the E-OBS dataset the 7-day period with maximum precipitation in each calendar year (with at least 30 years of annual data available). Increases of spring temperatures around or below the freezing point are considered a proxy for snow accumulation, melt and the transition from snowfall to rainfall. To understand the effect of these snowmelt processes on flood discharge, we calculated mean air temperature from January to April. When soil moisture is high, even small rainstorms may produce floods. To understand the effect of high soil moisture on floods, we identified for each grid point of the CPC Soil Moisture dataset the highest monthly soil moisture in each calendar year. We repeated the trend analyses for annual maximum precipitation, spring temperature, and annual maximum monthly soil moisture (Extended Data Fig. 5–7) on a 0.5° grid.

In the hotspot analyses, the time series for these three climate variables were extracted based on their location within the catchment boundaries (or within a buffer distance for small areas), from which Spearman's rank correlation coefficients (r) with the spatial medians of the original flood discharge series were calculated (Table 1). Confidence bounds at the 90% confidence level of r were estimated by stochastic block bootstrapping (*boot* package of R, random block size geometrically distributed with mean of 5 years) and are given in Extended Data Table 2b. The long-term evolution of the three climate variables were calculated and plotted in a similar fashion as those of the floods in Fig. 2.

We also analysed changes in the timing of the climate indices and floods as proxies for changing flood processes using previously established methods⁸ (Extended Data Fig. 4). The timing is used to interpret the process drivers of flood discharge changes. For Extended Data Fig. 4a, b, d the snow melt index is not shown, as it is of little relevance for flooding⁸.

To evaluate the relevance of the observed flood changes for flood management, the 100-year flood (Q_{100}) was estimated for each station using a Generalised extreme value (GEV) distribution

$$Q_T = \xi + \frac{\eta}{\kappa} \cdot \left[1 - (-\ln(1 - 1/T))^{\kappa} \right] \quad (5)$$

where Q_T is the T -year flood discharge. The parameters ξ , η and κ were estimated from the flood discharge series by Bayesian inference through an MCMC algorithm³⁹. Non-informative uniform prior distributions were used for ξ and $\log(\eta)$, while a normal distribution consistent with the geophysical prior⁴¹ were used for κ . 4000 parameter samples were drawn from the posterior distributions from which 4000 100-year floods were calculated for each station by Eq. (5). The median and the relative width of the 90% credible intervals are shown in Fig. 3. For comparability of the 100-year flood in catchments of different sizes, flood discharges per unit catchment area (specific flood discharges; $q_{100} = Q_{100}/A$, where A is catchment area) are shown.

If flood discharges change over time, the return period T may also change, e.g., the 100-year flood may become the 10-year flood if the flood discharges increase. Change in return period was therefore estimated by allowing the parameter ξ in Eq. (5) to change with time t as

$$\xi = a + b \cdot t \quad (6)$$

where the posterior distributions of a , b , η and κ were estimated from the flood discharge series by Bayesian inference through the same MCMC algorithm³⁹, using non-informative uniform prior distributions for a and b . More complex models than (6) were excluded because, for most of the stations, they did not outperform (6) based on the WAIC information criterion⁴². 4000 parameter samples were drawn from the posterior distributions from which 4000 100-year floods in 1960 were calculated for each station by Eqs. (5) and (6) with $t = 1960$. The changed return period in 2010 of

these 4000 flood peaks were computed by inverting Eq. (5) and by Eq. (6) with $t = 2010$. Finally, the median of the 4000 return periods was used as the 2010 return period of the 100-year flood discharge in 1960. Those stations where the 5th and the 95th percentiles of the uncertainty distribution agreed in the sign of change, were plotted as large points in Extended Data Fig. 8 while those where this was not the case were plotted as smaller points to indicate the uncertainty involved in the estimation.

To identify large-scale spatial patterns, the logarithms of the 2010 return periods of the 100-year flood discharge in 1960 were spatially interpolated using the *autoKrige* function³⁷ (Extended Data Fig. 8). For estimating the stationary 100-year specific flood discharge q_{100} (Eq. (5), Fig. 3), less stringent selection criteria (at least 30 years of data) than in all the other analyses were used as it can be estimated more robustly than trends and changes in the return period, which resulted in 3738 stations (Extended Data Fig. 1a).

In this paper we have analyzed flood discharge trends. The flood data set is freely available and can be used for a wide range of analyses.

Data Availability

The flood discharge data from the data holders/sources listed in Extended Data Table 1 that were used in this paper can be downloaded from Zenodo. The precipitation and temperature data from the E-OBS dataset can be downloaded from www.ecad.eu/download/ensembles/ensembles.php. The CPC soil moisture data can be downloaded from www.esrl.noaa.gov/psd.

Code Availability

The code for the trend and extreme value analyses can be downloaded from GitHub.

References Methods

31. Vogt, J. *et al.* A pan-European River and Catchment Database. European Commission, Joint Research Centre (2007).
32. Haylock, M. *et al.* A European daily high-resolution gridded data set of surface temperature and precipitation for 1950-2006. *J. Geophys. Res.* **113**, (2008).
33. Van den Dool, H., Huang, J. & Fan, Y. Performance and analysis of the constructed analogue method applied to US soil moisture over 1981-2001. *J. Geophys. Res.* **108**, (2003).
34. Sen, P. K. Estimates of the Regression Coefficient Based on Kendall's Tau. *J. Am. Stat. Assoc.* **63**, 1379–1389 (1968).
35. Theil, H. A Rank-invariant Method of Linear and Polynomial Regression Analysis, Part 1. *Proc. R. Neth. Acad. Sci.* **53**, 386–392 (1950).
36. Mann, H. B. Nonparametric tests against trend. *Econometrica: Journal of the Econometric Society*, 245-259 (1945).
37. Hiemstra, P. H., Pebesma, E. J., Twenhöfel, C. J. & Heuvelink, G. B. Real-time automatic interpolation of ambient gamma dose rates from the Dutch radioactivity monitoring network. *Comput. Geosci.* **35**, 1711–1721 (2009).
38. Helsel, D. R. & Frans, L. M. Regional Kendall Test for Trend. *Environ. Sci. Technol.* **40**, 4066–4073 (2006).
39. Renard, B., Lang, M. & Bois, P. Statistical analysis of extreme events in a non-stationary context via a Bayesian framework: case study with peak-over-threshold data. *Stoch. Env. Res. Risk A.* **21**, 97–112 (2006).
40. Wilcox, R. A note on the Theil - Sen regression estimator when the regressor is random and the error term is heteroscedastic. *Biometrical Journal: Journal of Mathematical Methods in Biosciences*, 40(3), 261-268 (1998).
41. Martins, E. S., & Stedinger, J. R. Generalized maximum-likelihood generalized extreme-value quantile estimators for hydrologic data. *Water Resources Research*, 36(3), 737-744 . (2000).

475 42. Watanabe, S. (2010). Asymptotic equivalence of Bayes cross validation and widely applicable
476 information criterion in singular learning theory. *Journal of Machine Learning Research*, 11,
477 3571-3594.

478
479

480 ACKNOWLEDGEMENTS

481 Supported by the ERC Advanced Grant “FloodChange” project (no. 291152), the Horizon 2020
482 ETN “System Risk” project (no 676027), the DFG “SPATE” project (FOR 2416), the FWF
483 “SPATE” project (I 3174), and a Russian Foundation for Basic Research (RFBR) project (no. 17-
484 05-41030 rgo_a). The data analysis was performed in R using the supporting packages *automap*,
485 *boot*, *lattice*, *maptools*, *ncdf4*, *plyr*, *raster*, *RColorBrewer*, *rgdal* and *rworldmap*. The authors also
486 acknowledge the involvement in the data screening process of C. Álvaro Díaz, I. Borzi, E.
487 Diamantini, K. Jeneiová, M. Kupfersberger, S. Mallucci and S. Persiano during their stays at the
488 Vienna University of Technology. We thank L. Gaál and D. Rosbjerg for contacting Finnish and
489 Danish data holders, respectively; B. Renard (France), W. Rigott (South Tyrol, Italy), G. Lindström
490 (Sweden) and P. Burlando (Switzerland) for assistance in preparing and/or providing data or
491 metadata from their respective regions. We acknowledge all flood data providers listed in Extended
492 Data Table 1.

493

494 Author contributions

495 G.B. and J.H. designed the study and wrote the first draft of the paper. G.B. initiated the study.
496 J.H. collated the database with the help of most of the co-authors, and conducted the analyses.
497 A.V. conducted the MCMC analysis. G.B., J.H., A.V., R.P., J.P. and B.M. interpreted the results in
498 the context of underlying geophysical mechanisms. J.P. compiled the catchment boundaries.
499 D.L. contributed to the statistical analysis. M.B., I.Č., A.K., S.K., O.L., M.M.-G., R.M., P.M., I.R.,
500 J.L.S., J.S. and N.Ž. interpreted the results in central Europe. G.T.A., A.B., O.B., M.B., A.C.,
501 G.B.C., P.C., D.G., A.M., L.M., M.Š., E.V. and K.Z. interpreted the results in southern Europe.
502 B.A., J.J.K. and D.W. interpreted the results in northern Europe. J.H., S.H., T.R.K., N.M., C.M. and
503 E.S. interpreted the results in western Europe. N.F., L.G., A.G., M.K., M.O. and V.O. interpreted
504 the results in eastern Europe. All authors contributed to framing and revising the paper.

505

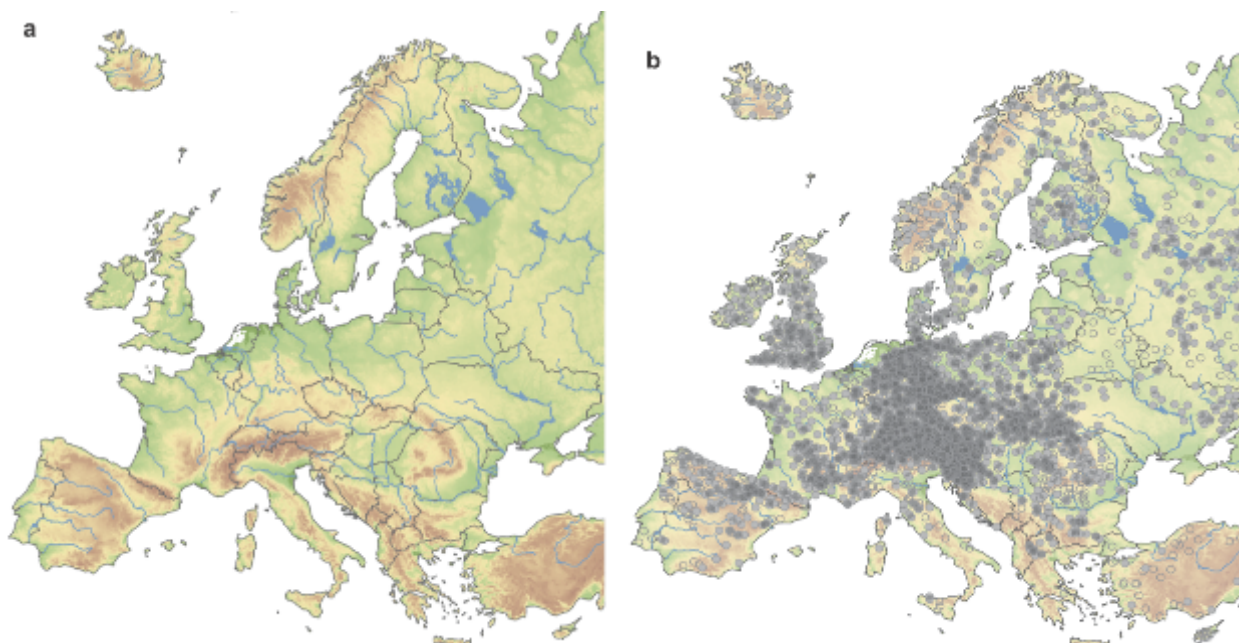
506 **Competing interests** The authors declare no competing interests.

507 **Correspondence** should be addressed to G.B. (bloeschl@hydro.tuwien.ac.at)

508

509 **Extended Data display items**

510



511

512

513

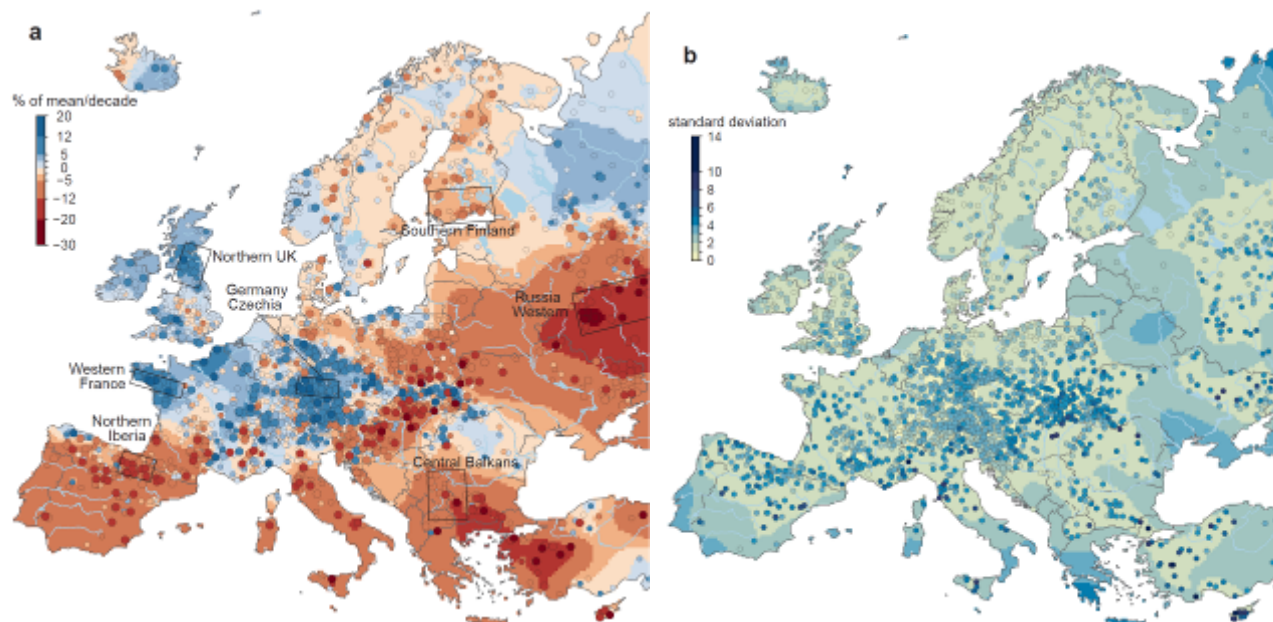
514

515

516

517

Extended Data Figure 1 | Map of European study area. (a) Elevation, main rivers and lakes and (b) location of the hydrometric stations analyzed. Open and full circles indicate stations with ≥ 30 years ($n = 3738$) and ≥ 40 years ($n = 2835$) of flood discharge data, respectively.



518

519

520

521

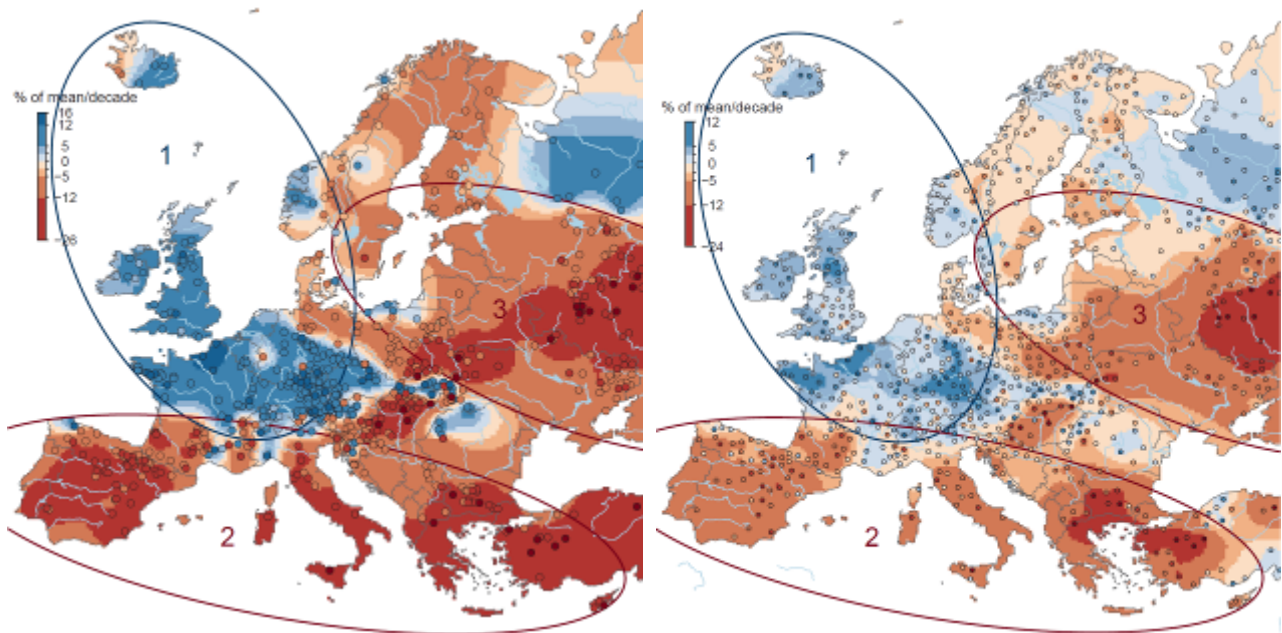
522

523

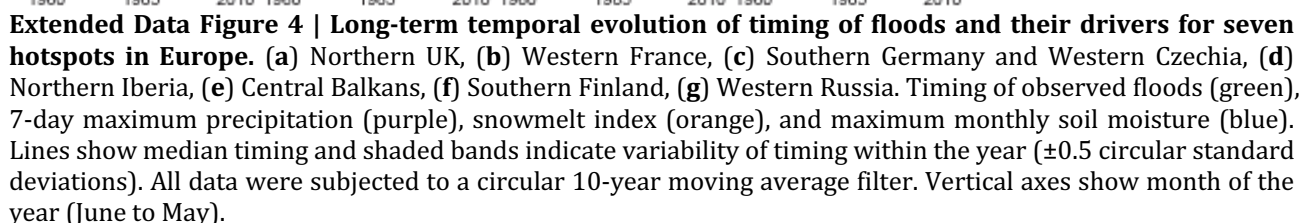
524

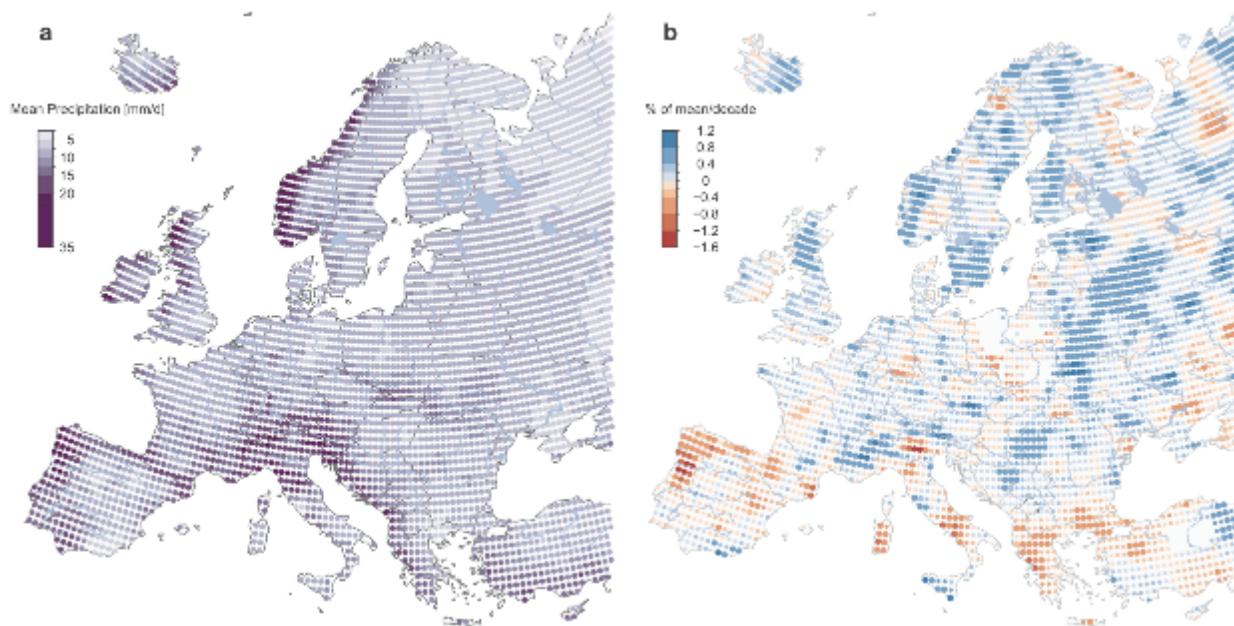
525

Extended Data Figure 2 | Observed trends of river flood discharges in Europe (1960–2010). (a) Points show local trends ($n = 2370$), where larger points indicate statistically significant trends ($\alpha = 0.1$). Background pattern represents regional trend. Blue indicates increasing flood discharges, red decreasing flood discharges. Rectangles indicate hotspot areas as in Fig. 2, Extended Data Fig. 3 and Extended Data Table 2c. (b) Uncertainties of the trends in terms of standard deviation. Points show local uncertainties. Background pattern represents regional uncertainties at the scale of a block size of 200×200 km. Units of both panels are % of mean/decade.



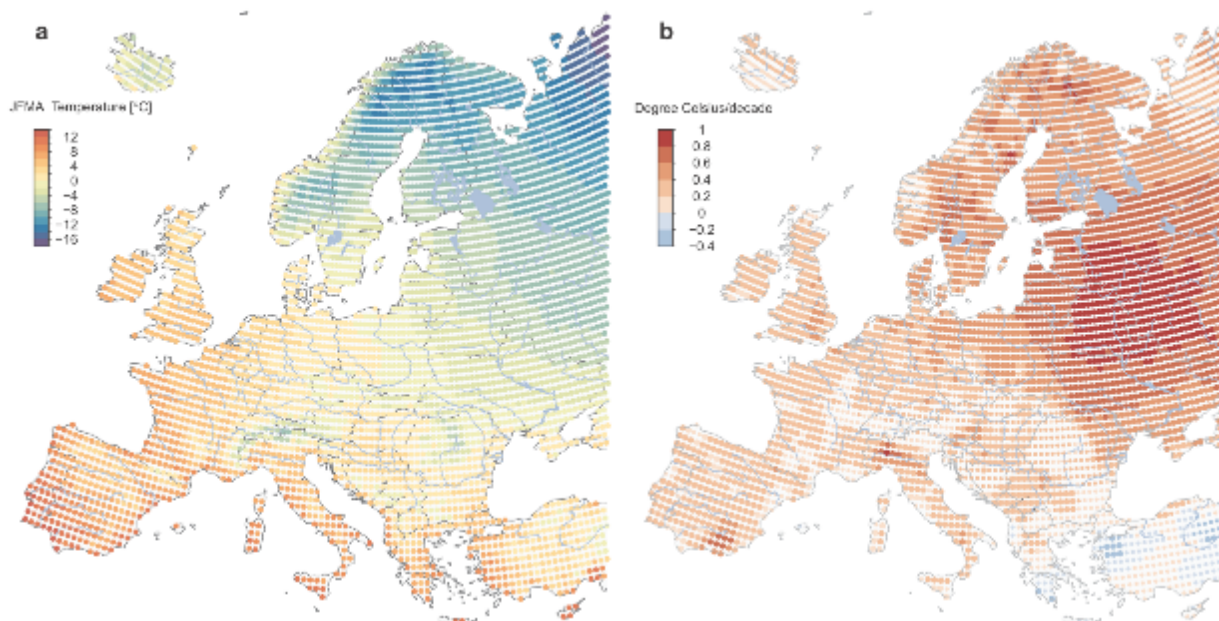
Extended Data Figure 3 | Flood trends as in Fig. 1 and Extended Data Figure 2, but using fewer stations.
 (a) Only stations with significant trends are used ($n = 664$). (b) Only stations with distances from each other larger than 50 km are used ($n = 745$).





Extended Data Figure 5 | 7-day maximum precipitation (1960–2010). (a) Long-term mean (mm/d); (b) trends in precipitation (% of mean per decade), where larger points indicate statistically significant trends ($\alpha = 0.1$); blue indicates increasing precipitation, red decreasing precipitation.

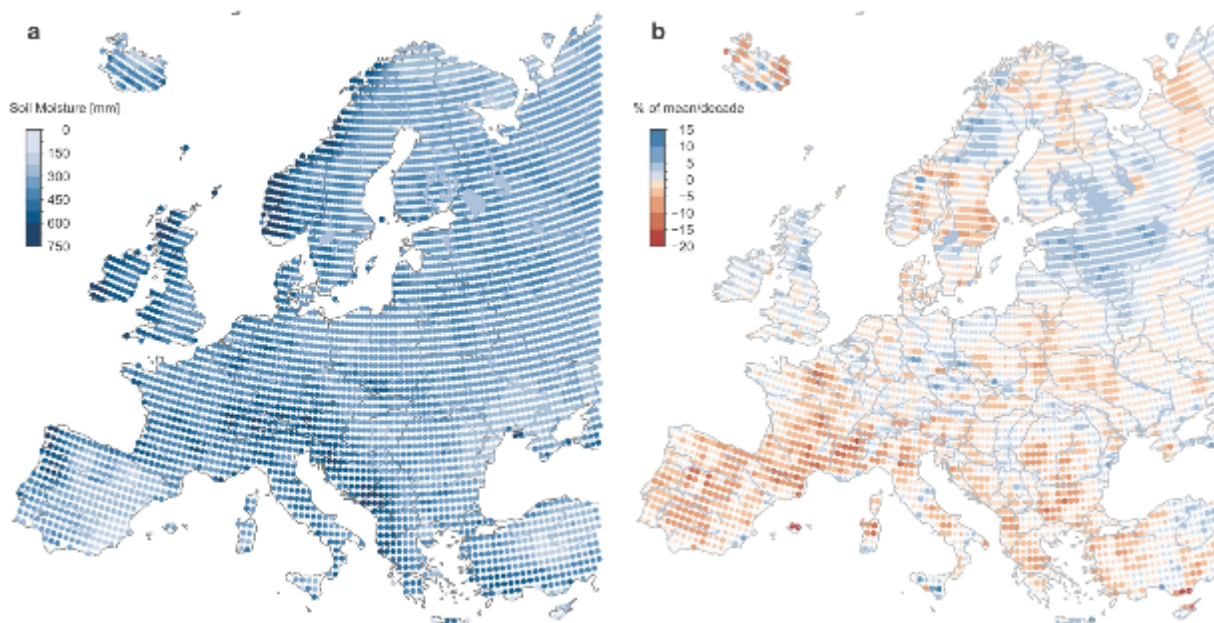
550
551



552
553
554
555
556

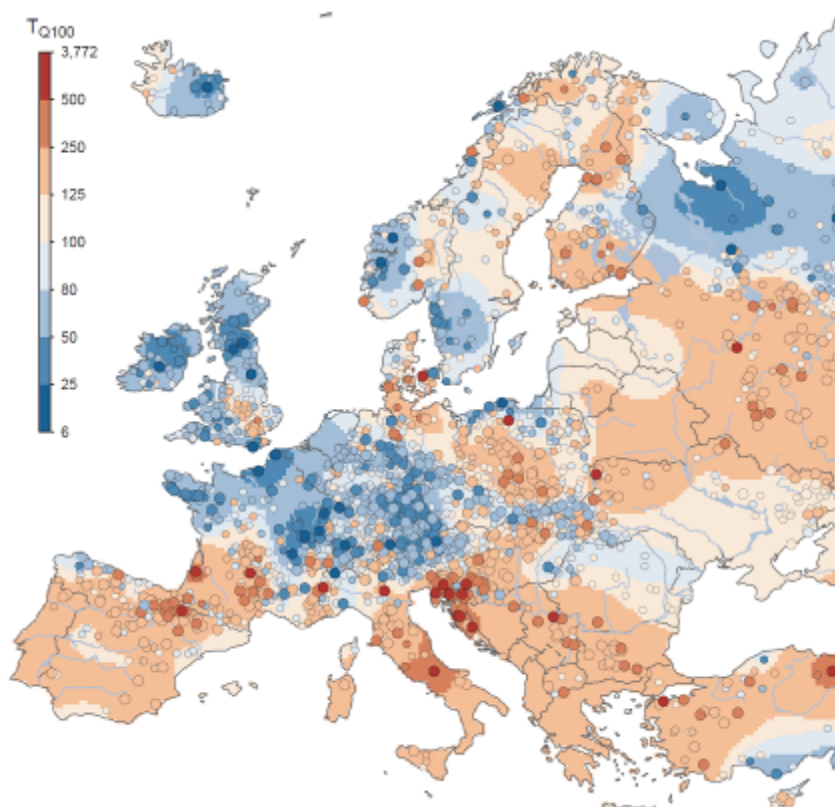
Extended Data Figure 6 | Spring (January to April) mean air temperatures (1960–2010). (a) Long-term mean (°C); (b) trends in temperatures (°C per decade), where larger points indicate statistically significant trends ($\alpha = 0.1$); red indicates increasing temperature, blue decreasing temperature.

557
558



559
560
561
562
563

Extended Data Figure 7 | Annual maximum monthly soil moisture (1960–2010). (a) long-term mean (mm); (b) trends in maximum soil moisture (% of mean per decade), where larger points indicate statistically significant trends ($\alpha = 0.1$); blue indicates increasing soil moisture, red decreasing soil moisture.



565
 566
 567
 568
 569
 570
 571
 572
 573

Extended Data Figure 8 | Estimated return period in 2010 of the discharge that was the 100-year flood in 1960. Points show local return periods ($n = 2370$), where larger points indicate agreement of the 5th and the 95th percentiles of the uncertainty distribution in the sign of change. Background pattern represents regional return periods. Blue indicates lower return periods representing increasing flood discharges, red indicates higher return periods representing decreasing flood discharges. This figure provides a continental overview, and does not replace national-scale and local studies where more detailed information may be available.

Extended Data Table 1 | Data Sources contained in the European Flood Research Database.

Country/Project	Data Holder/Source/Project information
Albania	National Hydro-Meteorological Service Albania, Institute of GeoSciences, Energy, Water and Environment (IGEWE)
Austria	Hydrographic Services of Austria (HZB)
Bosnia and Herzegovina	Hydrological Yearbooks of the former Republic of Yugoslavia
Bulgaria	Hydrological Yearbooks of the Rivers in Bulgaria, National Institute of Meteorology and Hydrology
Croatia	Meteorological and Hydrological Service of Croatia
Czechia	Czech Hydrometeorological Institute
Denmark	Danish Centre for Environment and Energy (DCE)
Estonia	Estonian Environment Agency
EWA	European Water Archive (EWA)
Finland	Finnish Environment Institute, Open information/Hydrology/Discharge, Source: SYKE
France	HYDRO database, French Ministry of Ecology, Sustainable Development and Energy
Germany	Federal Waterways and Shipping Administration (WSV)
Germany, Baden-Wuerttemberg	Ministry for the Environment, Climate and Energy of the Federal State of Baden-Wuerttemberg (LUBW)
Germany, Bavaria	Flood Information Centre, Bavarian Environment Agency, Munich (LfU)
Germany, Brandenburg	Ministry of Rural Development, Environment and Agriculture of the Federal State of Brandenburg (MLUL)
Germany, Hesse	Hessian Agency for Nature Conservation, Environment and Geology (HLNUG)
Germany, Lower Saxony	Lower Saxony Water Management, Coastal Defence and Nature Conservation Agency (NLWKN)
Germany, Mecklenburg-Western Pomerania	State Office of Environment, Nature Protection and Geology of Mecklenburg-Western Pomerania (LUNG)
Germany, North Rhine-Westphalia	State Agency for Nature, Environment and Consumer Protection (LANUV)
Germany, Rhineland-Palatinate	State Office for the Environment, Water Management and Commerce Inspectorate Rhineland-Palatinate (LUWG)
Germany, Saarland	The Saarland State Office for Environmental and Labour Protection (LUA)
Germany, Saxony	Saxon State Agency for Environment, Agriculture and Geology (LfULG)
Germany, Saxony-Anhalt	State Agency for Flood Defence and Water Management of Saxony-Anhalt (LHW)
Germany, Schleswig-Holstein	Schleswig-Holstein Agency for Coastal Defence, National Park and Marine Conservation (LKN.SH)
Germany, Thuringia	Thuringian Regional Office for the Environment and Geology (TLUG)
GRDC	The Global Runoff Data Centre, Koblenz, Germany
Greece	National Data Bank of Hydrological & Meteorological Information (NDBHMI)
Hungary	General Directorate of Water Management, Hungary
HYDRATE	EU-FP7 HYDRATE Project data base: Hydrometeorological Data Resources and Technology for Effective Flash Flood Forecasting
Iceland	Icelandic Meteorological Office, Hydrological Database, No. 2013-10-27/01
Ireland	Irish Environmental Protection Agency (EPA)
Ireland	Office of Public Works (OPW)
Italy	CUBIST database, former SIMN (Servizio Idrografico e Mareografico Nazionale)
Italy	National Research Council - Consiglio Nazionale delle Ricerche (CNR)
Italy	ENEL (Ente Nazionale per l'Energia Elettrica)
Italy	AdBPo (Autorità di Bacino del Fiume Po)
Italy	IRPI (Istituto di Ricerca per la Protezione Idrogeologica)
Italy	ISPRA (Istituto Superiore per la Protezione e la Ricerca Ambientale)
Italy, Emilia-Romagna Region	ARPA (Agenzia Regionale per la Protezione dell' Ambiente) Emilia-Romagna
Italy, Piedmont Region	ARPA Piemonte
Italy, Lazio Region	Ufficio Idrografico e Mareografico di Roma - Regione Lazio
Italy, Sicily Region	Osservatorio delle Acque della Regione Siciliana
Italy, South Tyrol Region	Hydrographic Office, Autonomous Province of Bolzano
Italy, Trentino Region	Dipartimento Protezione Civile, Provincia Autonoma di Trento
Italy, Umbria Region	Ufficio Idrografico - Regione Umbria
Italy, Veneto Region	ARPA Veneto
Latvia	Latvian Environment, Geology and Meteorology Centre, State Ltd.
Lithuania	Lithuanian Hydrometeorological Service
Macedonia	Macedonian Hydrometeorological Service
Netherlands	Rijkswaterstaat - Dutch Ministry of Infrastructure and the Environment
Norway	Norwegian Water Resources and Energy Directorate - Norges vassdrags- og energidirektorat (NVE)
Poland	Institute of Meteorology and Water Management National Research Institute (IMGW-PIB)
Portugal	Portuguese Environmental Agency - Agência Portuguesa do Ambiente, National Information System for Water Resources of Portugal (SNIRH)
Romania	National Institute of Hydrology and Water Management - NIHWM
Russia	The main hydrological characteristics, 1963-1970, 1971-75, 1975-1980, 1980-2000
Russia	Ministry of Natural Resources and Ecology of the Russian Federation, State Hydrological Institute
Russia	State Water Cadastre, 1985-2010, State Hydrological Institute, Lomonosov Moscow State University
Russia	Automated information system of state water bodies monitoring (AIS GMVO), Federal Agency for Water Resources
Serbia	Republic Hydrometeorological Service of Serbia (RHSS), Hydrological Yearbooks of Surface Water, Belgrade
Slovakia	Slovak Hydrometeorological Institute (SHMI)
Slovenia	Slovenian Environment Agency (ARSO)
Spain	Centre for Hydrographic Studies (Centro de Estudios Hidrográficos) of CEDEX, Spain
Sweden	Swedish Meteorological and Hydrological Institute (SMHI)
Switzerland	Federal Office for the Environment (FOEN) / (BAFU)
Turkey	General Directorate of Electrical Power Resources Survey and Development Administration (EIE), Turkey
Ukraine	Hydrological Department, Ukrainian Hydrometeorological Institute (UHMI)
Ukraine	Hydrometeorological Institute, Odessa State Environmental University (OSENU)
United Kingdom	UK National River Flow Archive (NRFA)

578
579
580

Extended Data Table 2a | Number of stations with positive and negative flood discharge trends. Regions according to Fig. 1.

		Positive Trend	Negative Trend	All
Europe	Significant $\alpha=0.1$	273 (11.52%)	391 (16.50%)	664 (28.02%)
	Not Significant	833 (35.15%)	837 (35.31%)	1706 (71.98%)*
	All	1106 (46.67%)	1228 (51.81%)	2370*
Region 1: North-western Europe	Significant $\alpha=0.1$	182 (20.34%)	27 (3.01%)	209 (23.35%)
	Not Significant	435 (48.60%)	240 (26.82%)	686 (76.65%)*
	All	617 (68.94%)	267 (29.83%)	895*
Region 2: Southern Europe	Significant $\alpha=0.1$	13 (2.84%)	142 (31.00%)	155 (33.84%)
	Not Significant	96 (20.96%)	169 (42.80%)	303 (66.16%)*
	All	109 (23.80%)	338 (73.80%)	458*
Region 3: Eastern Europe	Significant $\alpha=0.1$	5 (1.77%)	115 (40.78%)	120 (42.55%)
	Not Significant	54 (19.15%)	104 (36.88%)	162 (57.45%)*
	All	59 (20.92%)	219 (77.66%)	282*

[*stations with no trend included]

581
582
583
584
585
586

Extended Data Table 2b | Estimates and 90% confidence bounds (in brackets) of Spearman's rank correlation coefficient (r) between hotspot medians of the annual series of flood discharge and their drivers.

	Northern UK	Western France	Germany Czechia	Northern Iberia	Central Balkans	Southern Finland	Western Russia
Precipitation	0.70** (0.57, 0.76)	0.41* (0.15, 0.64)	0.40* (0.24, 0.56)	0.54** (0.39, 0.68)	0.22 (-0.11, 0.49)	0.08 (-0.11, 0.28)	-0.13 (-0.4, 0.18)
Soil Moisture	0.36* (-0.01, 0.66)	0.57** (0.39, 0.71)	0.56** (0.41, 0.68)	0.37* (0.12, 0.55)	0.68** (0.50, 0.76)	0.20 (0.01, 0.4)	0.30 (0.07, 0.49)
Spring temperature	0.09 (-0.15, 0.25)	0.5** (0.33, 0.63)	0.04 (-0.19, 0.23)	0.02 (-0.23, 0.32)	-0.29 (-0.44, -0.12)	-0.34 (-0.49, -0.15)	-0.55** (-0.7, -0.3)

[(**) p -value < 0.001, (*) p -value < 0.01]

587
588
589
590
591
592

Extended Data Table 2c | Flood discharge trends for selected hotspots (as % of station mean per decade). The significance level of the general hotspot trends is given according to the Regional Mann-Kendall test³⁸ with significance level α .

Hotspot Name	No. of Stations	Minimum trend	Maximum trend	Mean hotspot trend	Significance
Northern UK	15	2.9	12.5	6.6	$\alpha < 0.01$
Western France	16	5.9	17.6	9.7	$\alpha < 0.01$
Germany Czechia	47	1.6	17.8	8.0	$\alpha < 0.01$
Northern Iberia	34	-18.3	3.8	-8.3	$\alpha < 0.01$
Central Balkans	15	-17.6	-0.1	-8.4	$\alpha < 0.01$
Southern Finland	15	-10.0	-2.1	-5.2	$\alpha < 0.01$
Western Russia	21	-28.8	-8.3	-18.2	$\alpha < 0.01$

593
594
595
596